J Soils Sediments
DOI 10.1007/s11368-015-1266-4

SOILS, SEC 5 • SOIL AND LANDSCAPE ECOLOGY • RESEARCH ARTICLE

Multidisciplinary study of a Lateglacial-Holocene sedimentary sequence near Bologna (Italy): insights on natural and anthropogenic impacts on the landscape dynamics

Livia Vittori Antisari[1] · Gianluca Bianchini[2] · Stefano Cremonini[3] · Dario Di Giuseppe[2] · Gloria Falsone[1] · Marco Marchesini[4] · Silvia Marvelli[5] · Gilmo Vianello[1]

Received: 13 May 2015 / Accepted: 8 September 2015

Abstract
Purpose This study investigated a Lateglacial to Holocene sedimentary sequence derived from a small catchment located at San Lazzaro di Savena in the surroundings of Bologna Emilia (Northern Italy), in which different buried soil horizons were investigated in order to delineate the physiographic evolution of the area.
Materials and methods Several disciplinary/analytical approaches including pedostratigraphy, geochemistry, radiocarbon dating, archaeobotanical investigation and $\delta^{13}C$ stable isotopes analyses were taken into account for the pedosequence characterization.
Results and discussion This multidisciplinary approach allowed us to identify the main factors that affected the ancient environment over a prolonged time interval (~12 ky); starting from 14 ky BP with a palaeosol ascribed to the Bølling period, cold-arid conditions characterized by a steppic vegetation gradually evolved toward a more humid (and slightly warmer) setting. This climatic change allowed the development of a forest constituted by abundant conifers at ca 10 ky BP. Humans also impacted on the environment, at least since 9 ky BP, as indicated by repeated traces of firing (plausibly for deforestation and land clearance). The data allow a comparison with findings provided by other neighbouring sites and contribute to the ongoing debate on the relationships between climatic and anthropogenic impacts on the landscape dynamic.
Conclusions The human impact on the landscape has been effective from the Mesolithic, earlier than usually considered in previous studies. Anthropogenic activities caused geomorphological and hydraulic instabilities within the basin, accelerating soil erosion as indicated by the increase of the estimated sedimentation rates and change in the type of geochemical, mineralogical and textural properties of the studied soils.

Keywords ^{14}C dating and palynology · Archaeology and prehistoric fire · Climatic changes · Pedolology and geochemistry · $\delta^{13}C$ and carbon speciation

Responsible editor: Arnaud Temme

✉ Gianluca Bianchini
bncglc@unife.it

[1] Dipartimento di Scienze Agrarie, Alma Mater Studiorum-Università di Bologna, Via G. Fanin, 40, 40127 Bologna, Italy

[2] Dipartimento di Fisica e Scienze della Terra, Università di Ferrara, Via Saragat 1, 44100 Ferrara, Italy

[3] Scienze Biologiche, Geologiche e Ambientali, Alma Mater Studiorum-Università of Bologna, Via Zamboni 67, 40126 Bologna, Italy

[4] Soprintendenza Archeologica dell'Emilia-Romagna, Via delle Belle Arti 52, 40126 Bologna, Italy

[5] Laboratorio di Palinologia e Archeobotanica-C.A.A. Giorgio Nicoli, Via Marzocchi 17, 40017 San Giovanni in Persiceto, Bologna, Italy

1 Introduction

The interactions between anthropogenic activities and the environment have been correlated throughout human history. Since the early times, man has modified the environment (e.g. agriculture, grazing, use of fire) (Woodward 2009 and references within), but in turn some anthropogenic activities deeply influenced by climatic variability and environmental changes, as suggested by paleoenvironmental studies that hypothesized correlations between climate changes and cultural collapses (Mayewski et al. 2004; Diamond 2005; Bell and Walker 2005; Anderson et al. 2007; Weninger et al. 2009). In some cases, these correlations are strong and confirmed

Published online: 19 September 2015

along multiple lines, but in many other cases, correlations are weak and remaining untested and unconfirmed. For example, according to the current literature, Lateglacial-Holocene climate in Europe was punctuated by numerous short cooler events (Magny et al. 2006; Fleitmann et al. 2007; Yu et al. 2010; Wiersma and Jongma 2010; Miller et al. 2010; Giraudi et al. 2011) and these climatic changes were also recorded in some Mediterranean sites, even if their effects varied widely due to local microclimate factors (e.g. Joannin et al. 2013). The above-mentioned studies are mainly focussed on lake sediments, ice-records and speleothems, whereas other important archives such as soils are rarely taken into consideration.

Direct record of environmental changes have been rarely preserved in soils from mountain areas and large floodplains, while can be better highlighted in the foothill sedimentary sequences generated by streams having very small catchments. In this study, we investigated a Lateglacial-Holocene sedimentary sequence evolved from an aggradational alluvial fan at the outlet of a small catchment located in Emilia Romagna (Northern Italy), in which different buried soil horizons were detected. A multidisciplinary approach was carried out in order to assess the relative impact of climatic changes and possible anthropogenic activities in the study area. Our data give new insights for the scientific debate on the early role of human forcing on the environment. The topic is extremely important considering that recent findings highlight the reiterated presence of prehistoric human groups in the Emilia Romagna Region (Vittori Antisari et al. 2011; 2013). We show that detailed multiproxies investigations (including pedostratigraphy, geochemistry, radiocarbon dating, pollen and $\delta^{13}C$ stable isotopes analyses) are useful tools for the assessment of the factors that at local scale affected the ancient environment. We compared our results with those obtained from neighbouring sites in order to assess the hypotheses of early human impacts versus climate-vegetation dynamics at a regional scale. Therefore, the final goal of the paper is to investigate a soil sequence in order to provide more data and constraints on the ongoing debate on what happened in the transition between Lateglacial and Holocene and how human activities started to be effective on the environment and the landscape.

2 General setting

2.1 Geology and geomorphology

The study is focussed on a carefully cleaned section in the Municipality of San Lazzaro, 5 km eastward of Bologna (44°28′17″ N, 11°24′34″ E) at an elevation of 62 m above sea level (Fig. 1, point 1). It is located at the foothill of the Apennine hills and is crossed by the Via Emilia which is an important route since the Roman age. The investigation started in connection to a building excavation that reached the depth of ca 5.5 m, allowing careful field observations and sampling. From a geomorphological point of view, the site is located at the outlet of a little hilly catchment crosscut by a creek known as *Pontebuco stream*. The area consists of a gently sloping alluvial fan (hereon defined *Pontebuco stream fan*, PSF), 0.9 km^2 wide, hosted between the fan apexes of more important rivers such as Savena and Zena. Although the man-made modifications (post WW II) prevent a detailed recognition of minor landforms, in general the fan topographic surface does not show traces of bed entrenchment, suggesting an almost continuous aggradation of the fan structure. An older man-made feature on the fan is the prominent break in slope (ca 20 m/km) characterizing the northern roadway side of the Via Emilia, located less than 100 m south of the studied stratigraphic site (Fig. 1, point 1), due to the diachronic maintenance works performed on the ancient roman route. Upstream, the Pontebuco stream catchment is composed by the little valleys of two tributaries flowing mutually parallel. These tributaries are incised 15–30 m in the foothill and 70 m in the valley head. The catchment is about 3 km long and 0.5–0.6 km wide, with local widening related to ancient slide scars (Fig. 1). It is reasonable to think that the catchment inception could be dated at around 50–100 ky BP (Farabegoli et al. 1994), but it is unlikely that the most ancient PSF sedimentary phases can be recognized due to the sediment mixing with that of the major fans of neighbouring—considerably larger—rivers Savena and Zena.

From the geological point of view, the PSF apex is located precisely at the foothill hinge, where a vertical tilting is still developing, as result of the mountain chain rising coupled to the alluvial plain subsidence (Amorosi et al. 1996; Stramondo et al. 2007; Cremonini 2014). This narrow belt corresponds at depth to the buried Apennine chain main frontal thrust (Picotti et al. 1997; Picotti and Pazzaglia 2008; Martelli et al. 2009; Boccaletti et al. 2011).

Lithologically, PSF sediments are generally fine grained and the top of the gravel deposits, ascribed to the Last Glacial Maximum Savena-Zena fluvial system, is lying at ca 9 m below the topographic surface (Martelli et al. 2009). The understanding of sources of the fan sediments requires some information concerning the outcropping lithologies. The upper reach of the Pontebuco stream catchment (Fig. 1) is characterized by the outcrop of Pliocene-Lower Pleistocene marine clays (*Argille Azzurre Formation*, FAA) (Martelli et al. 2009) in turn overlain by a limited thickness of Lower-Middle Pleistocene littoral sands (*Sabbie di Imola* Formation, IMO) (Amorosi et al. 1998) outcropping down valley. In the foothill terraces zone (Fig. 1, point 3), these formations are in turn covered by variously weathered alluvial sediments (*Unità di Bazzano top*) that are 5–7 m thick.

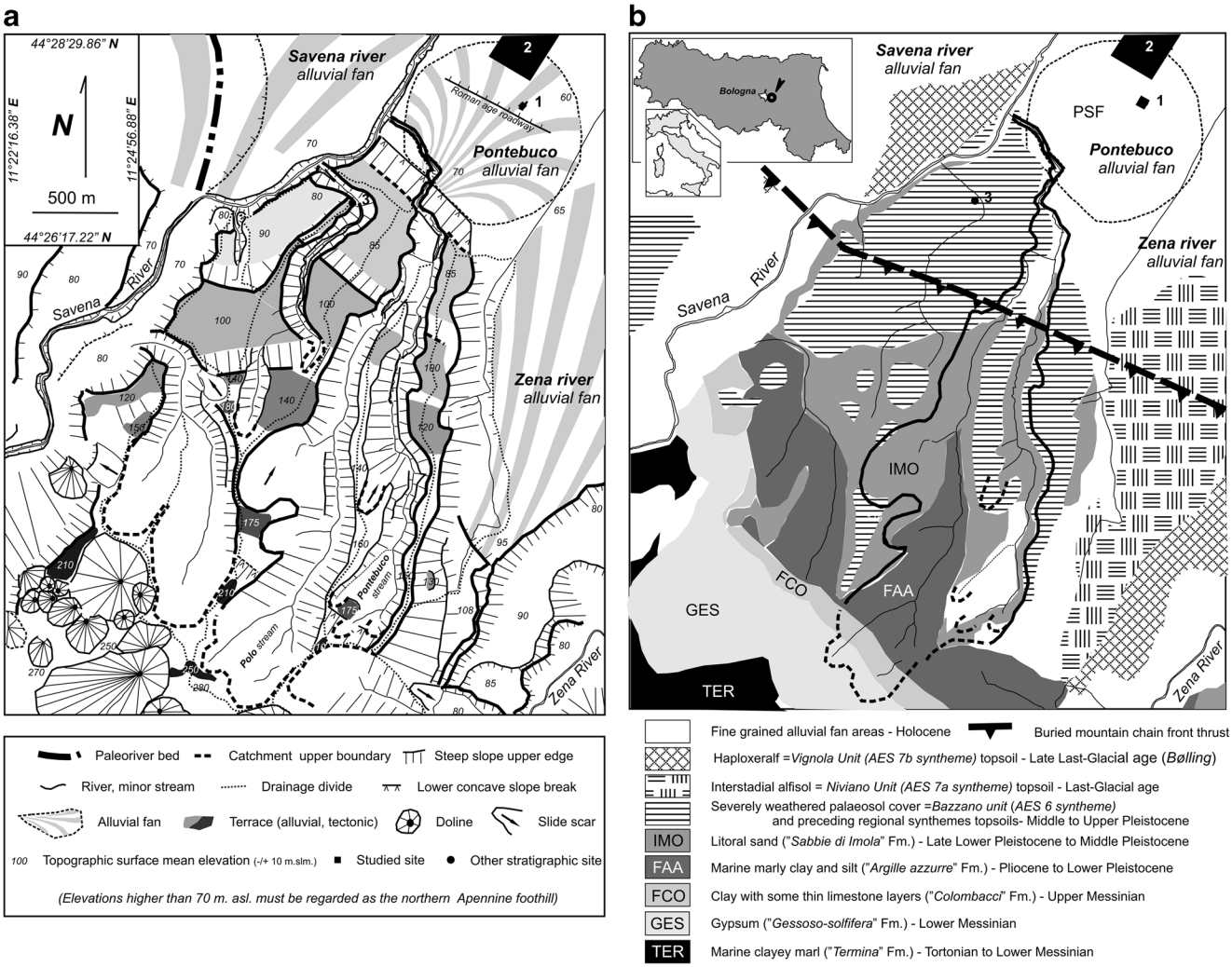

Fig. 1 **a** Geomorphological outline of the S. Lazzaro di Savena surrondings and related foothill. **b** Geological and pedological outline of the same area

2.2 Archaeology

The S. Lazzaro foothill physiographic environment is quite rich of archaeological findings spanning from the Palaeolithic to the protohistory (Nenzioni 1985). Outcrops preserving ancient traces of human activity (outcropping of lithic industries ranging from Palaeolithic to Chalcolithic) have been repeatedly recorded in the local alluvial sediments (Cremaschi 1987). The excavation performed in point 1 suggested the existence of topographic surfaces characterized by possible human frequentation, buried at 1.85, 3.47 and possibly at 4.75 m of depth, respectively (Fig. 2). The two deepest surfaces did not record any trace of significant archaeological materials (objects) but were characterized by posthole-like traces. The highest surface recorded some sherds probably dating to the Iron Age (Dr. G. Steffè, personal communication). These observations are consistent with those already recorded at point 2 (Fig. 1), located 200 m northward of the studied stratigraphic site, where a 76,000-m^2-wide brick-earth quarry (Fornace Galotti) removed the natural sediments up to a depth of more than 5 m allowing to recover archaeological artefacts spanning from the Palaeolithic up to the first Iron Age (Nenzioni 1985; Lenzi and Nenzioni 1996, Fig. 1: point 2). In particular, Villanovan Age graves were found at depth between 2 and 2.7 m, thus referring to a coeval ground surface buried at about 1.5 m of depth (Scarani 1963). The fan sediments also contain ex situ Palaeolithic materials relative to Clactonian and proto-Levallois lithic industries.

3 Materials and methods

3.1 Field observation and soil sampling

The field observation allowed the distinction of stratigraphic units and buried soil horizons which have been preliminarily characterized for layer-contact morphology, thickness, particle size distribution, colour and other textural characteristics. From the pedological point of view, the buried soils were described according to Schoeneberger et al. (2012) and a

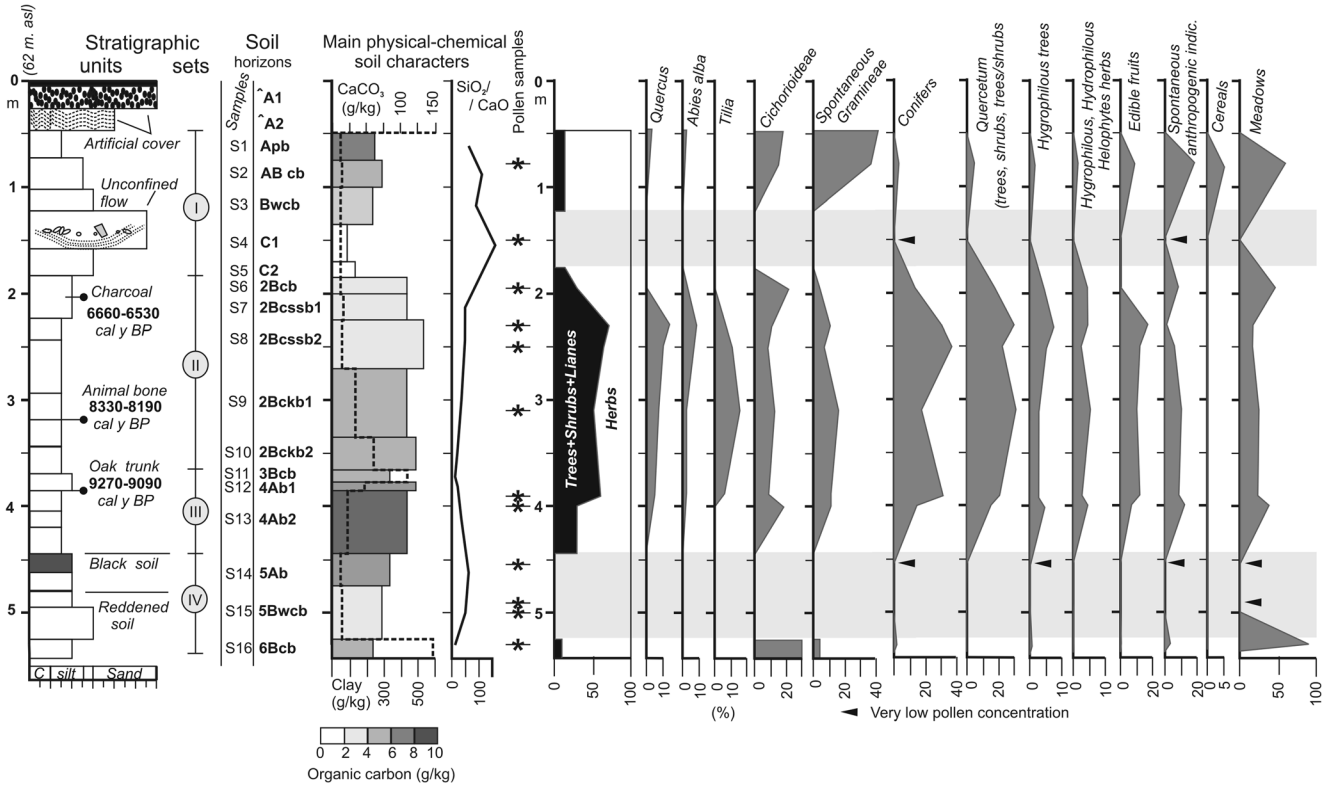

Fig. 2 Soil sequence coupled with selected parameters of the studied PFS site. In the *left*, distinct horizons have been grouped in four sets with precise indication of the sampling depths which have been constrained by radiocarbon datings. The *central part* of the figure reports description of the soil horizons in terms of clay, organic carbon and carbonate content and SiO_2/CaO ratio. On the *right*, vegetation constraints obtained by palynological investigations

sequence of 16 horizons has been recognized and sampled collecting about 1 kg of material from each horizon. A parallel sampling was performed for archaeobotanical (12 samples) and radiocarbon analyses (3 samples) as detailed below.

3.2 Soil analysis

The soil samples were air dried and sieved with a 2-mm-mesh sieve. The particle size distribution was determined by the pipette method after dispersion of the sample with a sodium hexametaphosphate solution (Gee and Bauder 1986). The pH value was potentiometric determined in a 1:2.5 (*w*/*v*) soil/distilled water suspension with a Crison pH meter. The electrical conductivity (EC) was also performed in a 1:2.5 (*w*/*v*) soil/distilled water suspension with an Orion conductivity meter. The carbonate content was measured by volumetric analysis of the carbon dioxide released by a 6 M HCl solution (Loeppert and Suarez 1996). The total organic C and N has been determined by an elemental CHNS-O EA 1110 Thermo Fisher Scientific; soil samples were weighted in silver pots and treated with HCl to eliminate the inorganic C.

Representative soil samples were selected for mineralogical characterization. The constituent mineralogical phases were identified by X-ray diffraction (XRD) by means of a Philips PW1860/00 diffractometer, using graphite-filtered CuKα radiation (1.54 Å). Diffraction patterns were collected in the 2θ angular range 3–50°, with a 5 s/step (0.02 2θ). Soil samples were also analyzed by X-ray fluorescence spectrometry (XRF) as described by Di Giuseppe et al. (2014). The technique enables the identification and quantification of major (SiO_2, TiO_2, Al_2O_3, Fe_2O_3, MnO, MgO, CaO, Na_2O, K_2O, P_2O_5, expressed in weight percent) and trace (Ba, Ce, Co, Cr, La, Nb, Ni, Pb, Rb, Sr, Th, V, Y, Zn, Zr, Cu, Ga, Nd and Sc expressed in mg kg^{-1}) elements. Samples (~10 g) were preliminarily quartered and then finely powdered using an agate mortar. Subsequently, an amount of about 4 g of powder was pressed with addition of boric acid by hydraulic press to obtain powder pellets. Simultaneously, 0.5–0.6 g of powder was heated for about 12 h in a furnace at 1000 °C in order to determine the Loss On Ignition (LOI) value. This parameter measures the concentration of volatile species contained in the sample. The analysis of the powder pellets was carried out using an ARL Advant-XP spectrometer, properly calibrated analysing certified reference materials. Precision and accuracy calculated by repeated analysis of numerous international standards having matrices comparable with those investigated, i.e. felsic igneous rocks such as granitoids (AC-E, G-2, GA, GH, GS-N, GSR-1, GSP-1) and rhyolites (JR3, RGM1),

and various typology of sedimentary rocks (JDO-1, JLK-1, JLS-1, JSD1, JSD2, JSD3), and were generally better than 3 % for Si, Ti, Fe, Ca and K, and 7 % for Mg, Al, Mn and Na. For trace elements (above 10 mg kg^{-1}), errors were generally better than 10 %.

Further investigations were obtained using an "Elemental, VARIO MICRO cube" analyser (combustion mode set at 950 °C) for the analysis of the weight percent of carbon coupled with an Isotopic Ratio Mass Spectrometer (IRMS) Isoprime100 for the analyses of the carbon isotope ratios ($^{13}C/^{12}C$). The carbon isotopic composition is given as δ‰ units, with respect to the values of notional standard, which is Pee Dee Belemnite (PDB): $\delta‰=(R_{sample}-R_{standard})/R_{standard}\times 1000$. The reproducibility and accuracy of spectrometric measurements were controlled by the repeated analyses of laboratory standards. The average $\delta^{13}C$ standard deviation was ±0.1‰ (Natali and Bianchini 2015). Analyses were repeated at combustion temperature of 450 °C to measure the carbon content and isotopic signature of the organic matter.

3.3 Radiocarbon dating (^{14}C)

The radiocarbon dating (^{14}C) was performed by high resolution mass spectrophotometry (AMS) technique. The method described by Calcagnile et al. (2005) and Fiorentino et al. (2008) included a preliminary treatment of the samples following a multi-step protocol that removed sources of contamination and converted material in graphite, the form suitable for AMS analyses. The carbon isotopic ratios were then analysed by comparing the ^{12}C and ^{13}C ion beam currents (and in turn the $^{13}C/^{12}C$ ratio expressed as $\delta^{13}C$) and the ^{14}C counts for the investigated samples with those obtained for reference materials (e.g., the fossil wood IAEA C4) of known isotopic composition supplied by the International Atomic Agency (IAEA). The conventional radiocarbon ages were calculated according to Stuiver and Polach (1977), and then converted to calendar ages by using the calibration dataset INTCAL04 (Blackwell et al. 2006) and the OxCal 3.1 software (Bronk Ramsey 2001).

3.4 Archaeobotanical analysis

3.4.1 Pollen analysis

Palynological analyses were carried out applying a methodology already tested for pollen substrates with some minor modifications (Lowe et al. 1996). The method includes the following phases: about 8–10 g was treated in 10 % Na-pyrophosphate to deflocculate the sediment matrix. A *Lycopodium* spores tablet was added to calculate pollen concentration (expressed as pollen grains per gram=p/g). The sediment residue was subsequently washed through 7-micron sieves and then resuspended in HCl 10 % to remove calcareous material and subjected to Erdtman acetolysis; heavy liquid separation method was then introduced using Na-metatungstate hydrate of s.g. 2.0 and centrifugation at 2000 rpm for 20 min. Following this procedure, the retained fractions were treated with 40 % HF for 24 h and then the sediment residue was washed previously in distilled water and after in ethanol with glycerol; the final residue was desiccated and mounted on slides by glycerol jelly and finally sealed with paraffin. This method preserves the slides for many years after preparation and therefore it is suitable for pollen extractions from geological and archaeological samples. Identification of the samples was performed at 1000 light microscope magnification (ocular ×10 and objective ×100). Determination of the pollen grains was based on the Palinoteca of our laboratory, atlases and a vast amount of specific morpho-palynological bibliography. Names of the families, genus and species of plants conform to the classifications of Italian Flora proposal by Pignatti (1982) and European Flora (Tutin et al. 1964–1993). The pollen terminology is based on Berglund and Ralska-Jasiewiczowa (1986), Faegri and Iversen (1989) and Moore et al. (1991) with slight modifications that tend to simplify nomenclature of plants. The term "taxa" is used in a broad sense to indicate both the systematic categories and the pollen morphological types (Beug 2004). Identified pollen groups have been expressed as percentages of the total (usually between 300 and 400 grains).

3.4.2 Microanthracological analysis

The same samples prepared for pollen analysis were also investigated for the identification of microcharcoals. Microanthracological analysis has been used to understand past fire events mostly connected to anthropogenic activities. Point count estimation of microscopic charcoal abundance was carried out, and charcoal fragments encountered during pollen counting were recorded in four size classes, based on long axis length (10–50, 50–125, 125–250, >250 μm) (Whitlock and Millspaugh 1996; Clark 1982, 1997; Patterson et al. 1987; Whitlock and Larsen 2001). The former two classes are thought to be wind-blown transported hence giving information concerning the regional fire events, whereas the latter two are considered the result of local vegetation burning.

3.4.3 Anthracological analysis

During the excavation, 26 carbonized trunks (from 30 to 50 years old) were found at 3.84 m depth (Fig. 2); in the field, subsamples were collected with a size of about 2.5–5.0 cm^3 for the identification. In the laboratory, they were identified using a reflected light microscope with the help to the anthraco-xylological reference collection and on the keys and atlases (Grosser 1977; Jacquiot et al. 1973; Schweingruber 1990; Hather 2000).

3.5 Statistical analysis

A multivariate statistical approach has been useful to summarize the multi-elementary chemical data provided by XRF of the considered horizons highlighting chemical analogies and differences between the samples, and delineating different sample groups. In this study, we used a combination of Principal Component Analysis (PCA) to correlate the measured parameters. A comprehensive mathematical/statistical description of the method is provided by Jolliffe (2002)). Through PCA, the observed elemental correlations were grouped in a small number of factors that account for most of the variance of the considered dataset. In particular, this elaboration was carried out by SPSS (Release 17.0, Lead Technologies, demo version), using Varimax with Kaiser Normalization as rotation method, as suggested by Facchinelli et al. (2001). On the basis of eigenvalues greater than one, four factors were selected for explaining 86.9 % of the cumulative total variance.

4 Results

Figure 2 synthesizes the results obtained in this study. More detailed information concerning the various type of data were reported in the distinct paragraphs reported below.

4.1 Soil sequence

Down to a depth of 5.5 m below ground level, the section divides into four main units, in which distinct soils have been recognized and described in Table 1 according to Schoeneberger et al. (2012).

The site showed a horizontal tabular layering very slightly dipping eastwards. The first set was recognizable down to the depth of 1.85 m, while the other three were separated by marked discontinuities at depths of 3.65, 4.45, and 5.25 m, respectively.

The uppermost set (including S1–S5 soil samples) consisted in a fining upward sequence with the sandy basal layer (35 cm thick) laterally continuous for tens of metres, possibly related to a splay deposit from an unconfined water current, thus resembling an alluvial fan lobe rather than a lateral crevasse splay. The sand layer contains granules and very small cherty pebbles suggesting that the clastic particles come from the *Sabbie di Imola* Formation (IMO; Fig. 1b). Some rounded fragments of Roman Age bricks were also found in the sand basal layer. The profile of this set was formed by the following horizons: Apb/ABcb/Bwcb/C1/C2 (from S1 to S5 soil samples; Fig. 2). The Bw horizon was recognized by both root sheaths and prismatic soil structures (Table 1), whereas C1 (S4) was a horizon with a natural high amount (50 %) of rounded rock fragment and a coarse (sand) texture. Below the lower limit (C2 soil horizons) of this set, a sharp lithological discontinuity was observed.

The second set (samples S6–S10), down 3.65 m, had a quite homogenous silty-clay texture (Table 1) and was characterized by a 2Bcb/2Bcssb1/2Bcssb2/2Bckb1/2Bckb2 sequence of horizons. Almost all the horizons were characterized by many mottles, a blocky angular structure, with sticky consistence, carbonate nodules/concretions and without skeleton. Hard breaking strength distinguished the dried samples that were also characterized by presence of slickenside (S7 and S8 layers) having at least 4 cm^2 extension; the S9 and S10 soil samples (corresponding to 2Bckb1and 2Bckb2 horizons) were characterized by pedogenetic carbonate nodules. At the boundary between S9 and S10, at the depth of 3.35 m, a bone fragment was found, while a charcoal useful for ^{14}C dating was sampled between 2Bcb and 2Bcssb1 (S6 and S7 soil samples, respectively; Fig. 2).

The third set (down to 4.45 m of depth) consisted of variously darkened layers (S12 and S13) and its upper limit was marked by the lithological discontinuity in the 3Bcb horizon (S11 soil sample). The 3Bcb horizon was characterized by the presence of carbonate masses of primary origin (i.e. residues of the parent material). The S12 and S13 layers were coded as 4Ab1 and 4Ab2 due to the textural change with marked increase in the clay content (silty-clay texture; Table 2) with respect the overlying horizon, highlighting the presence of another lithological discontinuity; furthermore, some features like a dark colour (10YR5/3 and 10YR4/2, respectively), hard consistence and plastic character and also carbonate masses and concretions were observed. A burnt tree was sampled between these two horizons.

The fourth set (down to the bottom of the excavation, including S14–S15 samples) was characterized by a change of texture (clay-loam) identifying a further lithological discontinuity. Granular structure, dark colour (10YR3/3) and mottles (10YR5/6) characterized the S14 horizon, whereas S15 showed reddish colour (2.5Y6/6) with mottles (10YR6/8) and a subangolar blocky structure. These features suggested 5Ab and 5Bwcb horizons sequence, respectively. In the deepest S16 horizon, an additional discontinuity marked by a further change in the texture (loam) was detected. Yellowish brown colour, with presence of mottles (10YR6/8) and carbonate nodules allowed to code this horizon as 6Bwcb (Fig. 2 and Table 2).

4.2 Physical-chemical soil properties

Table 2 shows the main physicochemical soil properties. The pH values ranged from 7.6 to 8.2; generally, the total carbonate content was low (from 9 to 60 g kg^{-1}), increasing only in the horizons marking sharp lithological discontinuities (103 and 153 g kg^{-1} for S11 and S16, respectively). The organic C content ranged from 1.4 to 8.3 g kg^{-1}; the C1 and C2 layers

Table 1 Main descriptive elements of investigated soil profiles. Codes according to Schoeneberger et al. (2012)

Stratigraphic set	Sample	Horizons				Munsell colour		Mottles					Texture	Structure	Consistence	Concentrations	Rock and other fragments	
		Horizon	Depth (cm)	Boundary														
				D	T	Dry	Moist	Q	S	C	Colour	M		G_S_T	D_M_S_P	Q_S_K	V%	R
	Not collected	^A1	0–30	A	S								SL					
		^A2	30–50	A	S								SL					
I	S1	Apb	50–75	C	S	10YR 6/3	10YR 5/3	–	–	–	–	–	L	3_m_pl	SH_FR_(w)ss_(w)ps	–	1	SR
	S2	ABcb	75–100	D	S	10YR 6/4	10YR 5/4	vf	1	F	10YR 5/6	d	CL	3_m_pr	SH_FR_(w)ss_(w)ps	f_1_RSB	0	–
	S3	Bwcb	100–135	A	S	10YR 6/6	10YR 5/4	f	1	F	10YR 5/6	d	L	3_m_pr	HA_FI_(w)ss_(w)ps	f_1_RSB	2	SR
	S4	C1	135–170	G	S	10YR 6/6	10YR 6/8	–	–	–	–	–	SL	0_f_sg	SH_FR_(w)so_(w)po	f_1_CBM	50	RO
	S5	C2	170–185	C	S	10YR 7/4	10YR 6/6	c	1	F	10YR 5/8	d	L	3_m_abk	HA_FI_(w)so_(w)po	f_1_DNN	3	RO
II	S6	2Bcb	185–201	C	S	2.5Y 6/4	2.5Y 4/2	m	1	P	7.5YR 6/8	d	SiC	2_f_abk	VH_FI_(w)ss_(w)vp	c_1_RSB	0	–
	S7	2Bcssb1	201–225	C	S	2.5Y 6/2	2.5Y 4/2	m	1	D	2.5Y 5/4	d	SiC	2_f_abk	VH_FI_(w)ss_(w)ps	c_1_CAN	0	–
	S8	2Bcssb2	225–271	C	S	2.5Y 6/3	2.5Y 4/2	m	3	D	10YR 5/6	d	SiC	2_m_abk	VH_FI_(w)ss_(w)ps	c_1_CAC	0	–
	S9	2Bckb1	271–335	C	S	2.5Y 5/4	10YR 4/3	c	2	F	5YR 3/2	d	SiC	2_m_abk	VH_FI_(w)s_(w)p	c_2_CAN	2	RO
	S10	2Bckb2	335–365	A	W	10YR 5/3	10YR 3/3	m	4	D	G 2 8/5B	d	SiC	3_m_pr	HA_VFR_(w)ss_(w)vp	c_1_CAC/SFB	2	RO
III	S11	3Bcb	365–377	A	W	10YR 7/3	10YR 4/3	–	–	–	–	–	SiCL	2_f_abk	HA_FR_(w)vs_(w)ps	c_2_CAM/RSB	2	RO
	S12	4Ab1	377–385	C	W	10YR 5/3	10YR 3/3	–	–	–	–	–	SiC	3_m_abk	EH_EF_(w)s_(w)p	c_1_CAC	0	
	S13	4Ab2	385–445	C	W	10YR 4/2	10YR 3/2	–	–	–	–	–	SiC	3_f_abk	VH_VFI_(w)ss_(w)vp	m_2_CAM	0	
IV	S14	5Ab	445–475	C	W	10YR 3/3	10YR 3/2	f	1	F	10YR 5/6	d	CL	2_f_gr	SH_VFR_(w)so_(w)ps	m_2_CAM	5	SR
	S15	5Bwcb	475–525	C	W	2.5Y 6/6	2.5Y 4/4	m	2	F	10YR 6/8	d	CL	2_m_sbk	HA_VFR_(w)s_(w)vp	m_2_CAN	2	SR
	S16	6Bcb	525–545	U		2.5Y 6/4	10YR 5/4	f	2	D	10YR 6/8	d	L	2_f_abk	VH_FR_(w)s_(w)p	c_1_CAN	0	

Horizon boundary. (D) Distinctness: A=abrupt, C=clear, G=gradual, D=diffuse; (T) topography: S=smooth, W=wavy, U=unknown. Mottles. (Q) Quantity: vf=very few, f=few, c=common, m=many; (S) size: 1=fine, 2=medium, 3=coarse, 4=very coarse; (C) contrast: F=faint; D=distinct; P=prominent; (M) moisture state: d=dry; texture. Field estimation: SL=sandy loam, L=loam, SiCL=silty clay loam, SiC=silty clay, CL=clay loam. Structure. (G) Grade: 0=structureless/very weak, 1=weak, 2=moderate, 3=strong; (S) size: vf=very fine, f=fine, m=medium, c=coarse; (T) type: gr=granular, abk=angular blocky, sbk=subangular blocky, pr=prismatic, pl=plat, sg=single grain. Consistence. Rupture resistence: (D) dry: SH=slightly hard, HA=hard, VH=very hard, EH=extremely hard; (M) moist: VFR=very friable, FR=friable, FI=firm, VFI=very firm, EF=extremely firm; (S) stickiness: (w)so=non-sticky, (w)ss=slightly sticky, (w)s=moderately sticky, (w)vs=very sticky; (P) plasticity: (w) po=non-plastic, (w) ps=slightly plastic, (w)p=moderately plastic, (w)vp=very plastic. Concentrations. (Q) Quantity: f=few, c=common, m=many; (S) size: 1=fine, 2=medium, 3=coarse; (K) kind: CAC=carbonate concretions, CAM=carbonate masses, CAN=carbonate nodules, CBM=clay bodies, DNN=durinodes-SiO_2, RSB=root sheaths, SFB=shell fragments. Rock and other fragments. (K) Kind: SHF=shell (V%) Fragment content % by volume; (R) roundness: SR=subrounded, RO=rounded

Table 2 Chemical-physical characters of the investigated soil profiles

Stratigraphic set	Sample	Horizon	Depth cm	pH (H_2O)	EC	Texture					$CaCO_3$	TOC	TN
					mS/cm 20 °C	Sand G g kg^{-1}	Sand F	Silt G	Silt F	Clay	g kg^{-1}		
I	S1	Apb	50–75	7.6	207	87	268	132	264	249	9	6.2	0.9
	S2	ABcb	75–100	7.7	142	60	222	94	328	296	11	4.1	0.7
	S3	Bwcb	100–135	7.7	197	140	347	109	173	231	9	2.4	0.5
	S4	C1	135–170	7.8	164	526	280	33	51	109	10	1.4	0.4
	S5	C2	170–185	7.6	135	124	372	157	170	177	9	1.6	0.5
II	S6	2Bcb	185–201	7.9	157	16	95	99	338	452	11	4.8	09
	S7	2Bcssb1	201–225	8.0	240	26	80	53	381	460	18	3.0	0.6
	S8	2Bcssb2	225–271	8.1	240	15	56	39	365	525	18	3.6	0.6
	S9	2Bckb1	271–335	8.0	244	10	70	44	400	475	33	4.3	0.9
	S10	2Bckb2	335–365	8.0	274	31	51	21	393	503	60	5.2	0.7
III	S11	3Bcb	365–377	8.2	263	41	145	176	312	326	103	4.1	0.6
	S12	4Ab1	377–385	8.1	243	14	96	86	332	472	46	6.8	0.8
	S13	4Ab2	385–445	8.0	243	9	142	113	287	449	19	8.3	1.1
IV	S14	5Ab	445–475	7.8	216	9	241	183	269	297	10	6.7	0.9
	S15	5Bwcb	475–525	7.9	215	20	233	204	271	271	15	4.0	0.7
	S16	6Bcb	525–545	8.2	235	58	230	183	289	240	153	4.1	0.7

had the lowest organic C amount <2 g kg^{-1}, whereas the highest organic C content was detected in the lowest Ab horizons (S12, S13 and S14 samples coded as 4Ab1, 4Ab2 and 5Ab horizons, respectively).

The box plots of Fig. 3, obtained for the different sets of samples recognized along the stratigraphy, show an increase of pH values in the second and third sets, associated to a slight increase of carbonate. An increase of organic C and total N along the depth of sequence is also noticed. The sand and clay contents confirmed the existence of lithological discontinuities already observed during the field survey.

The mineralogical composition of the first three sets has been investigated by XRD. In the most superficial set (sample S2), the dominant mineral phase was quartz, with only minor sporadic amount of calcite and phyllosilicates, whereas in the second (sample S8) and third (sample S12) sets, the amount of quartz decreased, while calcite and phyllosilicates progressively increased (Fig. 4).

The geochemical composition expressed by the amount of major and trace elements (Table 3) reflected the differences in the mineralogical composition observed in the distinct sets. Elaboration of these data by PCA highlighted the geochemical

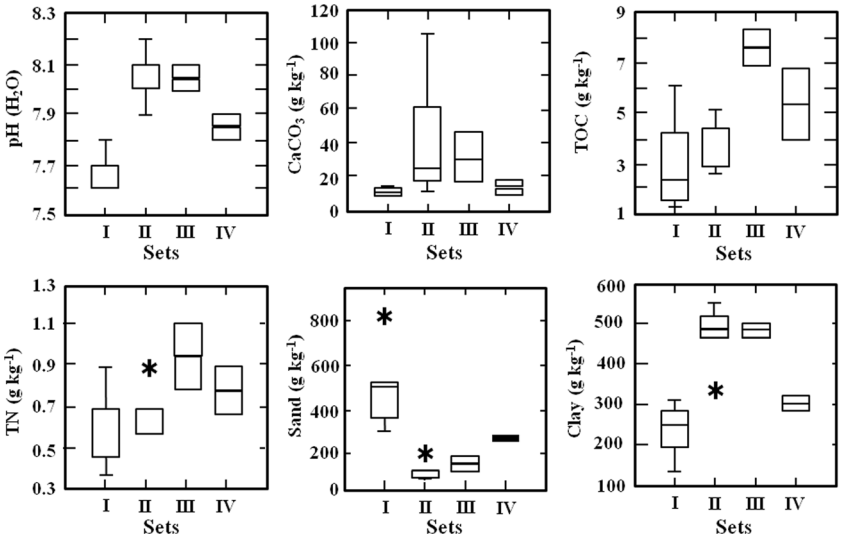

Fig. 3 Box plot showing textural and physicochemical parameters of the different sets of horizons: *I* includes samples 1, 2, 3, 4, 5; *II* includes samples 6,7,8,9 10; *III* includes samples 11, 12 13; *IV* includes samples 14 and 15

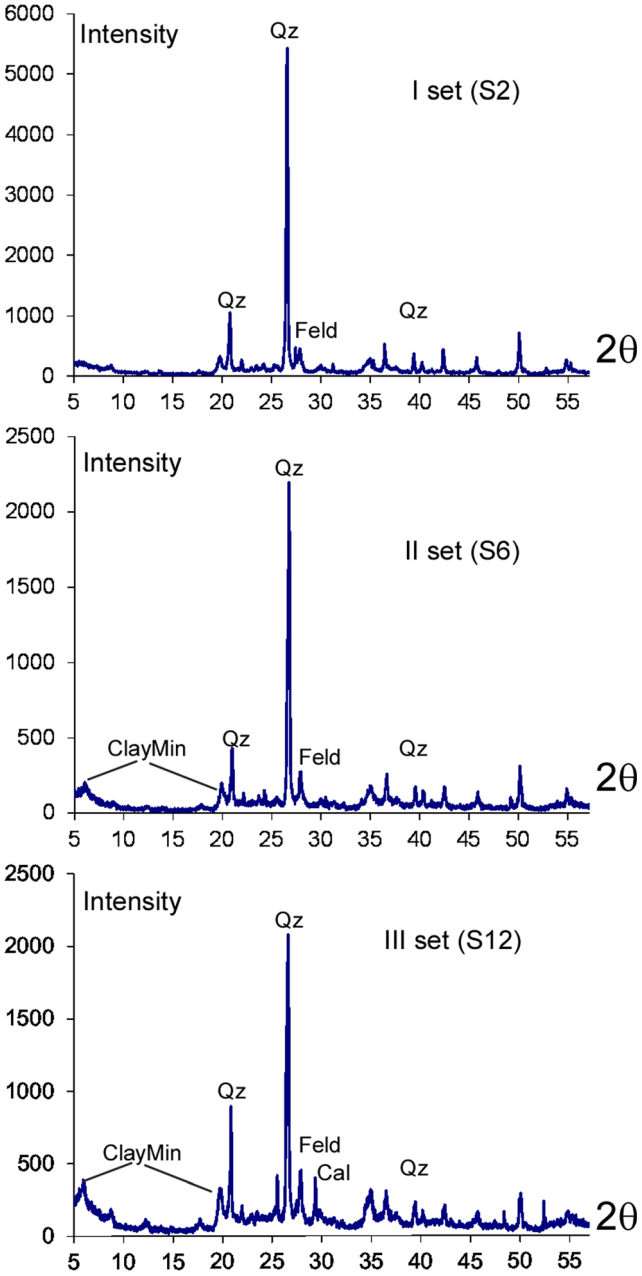

Fig. 4 XRD analyses of soil samples representative of three excavation levels. Note that the more superficial sample 1 records only quartz (preponderant) and feldspar (subordinate), whereas deeper levels (6 and 12 samples) also record the presence of clay minerals. Calcite seems abundant only in the deeper horizons

analogies and differences between soil samples of the distinct sets. In fact, the defined sets broadly corresponded to homogeneous families having distinctive geochemical features (Fig. 5), suggesting that the pedological sequence ranging from S1 to S5 had a homogeneous geochemical affinity. A second homogeneous family extended from the layers S6 to S10. The deeper part of the excavation was less homogeneous, and from the geochemical point of view, differences between S12–S13 and S14–S15 horizons were observed.

High content of quartz fitted with the very high SiO_2 content (65–78 wt%) of the first set, and comparatively low Al_2O_3 (<15.8 wt%) and CaO (<0.95 wt%) percentage confirmed the low amount of phyllosilicates (such as clay minerals) and very low carbonate content. The second set, from S6 to S10 samples, was totally different from the more superficial first set due to the lower SiO_2 content (55.3–61.1 wt%) and higher Al_2O_3 and CaO amount (15.8–17.8 and 1.0–6.1 wt%, respectively), thus confirming the greater content of phyllosilicates and calcite that was recorded by XRD. The soil samples of this set were also enriched in many trace elements such as Ni, V, Sc, Rb, Ba, La, Nd, Th and Nb (Table 3; Fig. 6) that can be hosted by phyllosilicates such as smectite, chlorite and other accessory femic minerals. Within the second set, SiO_2 percentage decreased systematically from the most superficial horizon (2Bcb) to the deepest one (2Bckb2), whereas, in contrast, CaO (and Sr) content increased.

The difference in SiO_2, Al_2O_3 and CaO between S12–S13 (55.4–58.2, 17.7–17.8 and 1.6–3.0 wt% for S12 and S13, respectively) and S14–S15 samples (61.9–62.8, 16.4–16.9, 1.3–1.5 wt%, for S14 and S15, respectively) suggested that these horizons belonged to distinct sedimentary phases. The trace element distribution (Fig. 6) seemed to further support this interpretation.

The deepest investigated sample (S16) seemed a further independent soil, which reflected a significant presence of geogenic carbonates testified by very high Ca and Sr content.

The elemental-isotopic results of both total C (C_{tot}) and organic C (C_o) carried out on the studied pedostratigraphic sequence are reported in Table 4 and Fig. 7. C_o should complement the inorganic carbon fraction C_i (that can be inferred from the $CaCO_3$ content of Table 2) and the sum of two fractions (C_o+C_i) should be equal to the measured C_{tot} as following: $C_o+C_i=C_{tot}$. It can be observed that the C_{tot} content varied between 0.9 and 2 wt%, while the related $\delta^{13}C$ ranged between −11.4 and −24.7‰ (Table 1). These C_{tot} isotopic values result from the mixing of organic matter (usually characterized by strongly negative isotopic values) and carbonates which were characterized by $\delta^{13}C$ ~0‰. Coherently, the less negative isotopic values marked perfectly the carbonate-rich horizons. The carbon isotopic composition of the organic fraction had a much more homogeneous $\delta^{13}C$ between −23.6 and −25.2‰.

A misfit between the measured C_{tot} and the calculated one (C_o+C_i) was also investigated, and this deficiency (ΔC) was recorded in the most superficial S1 horizon and in the horizons S12, S13, S14. This parameter highlighted the presence of a further carbon fraction that was not recorded, plausibly represented by black (elementary) charred carbon. The elementary carbon detected in the deep S12, S13, S14 was probably related to fires and biomass burning (i.e. burnt trees).

Table 3 Concentration of major and trace elements obtained by XRF

	Sample	Horizon	Depth cm	SiO_2 wt%	TiO_2	Al_2O_3	Fe_2O_3	MnO	MgO	CaO	Na_2O	K_2O	P_2O_5	LOI
	S1	Apb	50–75	67.81	0.63	14.14	6.33	0.13	1.81	0.94	1.05	2.67	0.28	4.21
	S2	ABcb	75–100	65.47	0.70	15.75	7.31	0.16	2.03	0.61	0.93	2.86	0.11	4.07
I	S3	Bwcb	100–135	69.93	0.53	14.38	5.59	0.11	1.55	0.72	1.20	2.82	0.09	3.09
	S4	C1	135–170	77.89	0.29	10.59	4.14	0.09	0.78	0.38	1.28	2.75	0.09	1.72
	S5	C2	170–185	69.99	0.60	14.19	6.02	0.16	1.60	0.65	1.21	2.76	0.09	2.74
	S6	2Bcb	185–201	61.06	0.79	17.53	8.58	0.07	2.36	1.02	0.68	2.60	0.07	5.24
	S7	2Bcssb1	201–225	59.32	0.78	17.46	8.69	0.12	2.50	1.70	0.63	2.59	0.07	6.14
II	S8	2Bcssb2	225–271	57.93	0.80	17.86	9.32	0.11	2.68	1.43	0.56	2.70	0.08	6.53
	S9	2Bckb1	271–335	57.49	0.80	17.30	8.94	0.10	2.65	2.27	0.59	2.68	0.10	7.09
	S10	2Bckb2	335–365	55.35	0.78	17.37	8.92	0.11	2.71	3.02	0.52	2.82	0.11	8.27
	S11	3Bcb	365–377	55.14	0.73	15.83	7.27	0.10	2.36	6.07	0.69	2.79	0.13	8.89
III	S12	4Ab1	377–385	55.43	0.78	17.67	8.67	0.10	2.68	3.00	0.55	3.11	0.15	7.85
	S13	4Ab2	385–445	58.15	0.77	17.77	8.53	0.11	2.68	1.57	0.63	3.18	0.13	6.48
	S14	5Ab	445–475	62.81	0.75	16.41	7.44	0.13	2.36	1.34	0.98	3.00	0.12	4.66
IV	S15	5Bwcb	475–525	61.87	0.73	16.85	7.79	0.12	2.69	1.50	1.02	2.79	0.14	4.50
	S16	6Bcb	525–545	54.75	0.64	13.51	5.85	0.11	2.41	9.29	0.95	2.46	0.14	9.90

Strat. set	Sample	Horizon	Depth cm	Ba mg kg^{-1}	Co	Cr	Cu	Ga	Hf	La	Nb	Nd	Ni
	S1	Apb	50–75	398	21	121	81	16	10	65	11	30	64
	S2	ABcb	75–100	396	22	148	34	18	11	73	12	29	90
I	S3	Bwcb	100–135	404	20	139	25	14	9	63	9	26	58
	S4	C1	135–170	373	14	230	23	10	9	56	6	15	37
	S5	C2	170–185	382	22	149	24	15	12	74	12	29	69
	S6	2Bcb	185–201	439	22	156	37	23	10	81	14	35	83
	S7	2Bcssb1	201–225	449	24	167	39	24	9	83	14	32	110
II	S8	2Bcssb2	225–271	440	25	176	44	26	10	81	17	35	123
	S9	2Bckb1	271–335	443	22	164	44	26	11	75	15	33	110
	S10	2Bckb2	335–365	435	22	167	47	27	9	83	19	33	118
	S11	3Bcb	365–377	422	19	113	40	22	8	72	13	26	77
III	S12	4Ab1	377–385	456	22	143	45	26	9	74	13	37	96
	S13	4Ab2	385–445	469	23	138	42	26	11	71	17	34	88
	S14	5Ab	445–475	465	20	132	34	20	14	76	15	28	73
IV	S15	5Bwcb	475–525	461	21	149	33	21	13	77	13	31	88
	S16	6Bcb	525–545	381	19	118	29	18	8	65	13	22	77

Strat. set	Sample	Horizon	Depth cm	Pb mg kg^{-1}	Rb	S	Sc	Sr	Th	V	Y	Zn	Zr
	S1	Apb	50–75	41	112	6	12	111	4	76	19	93	202
	S2	ABcb	75–100	21	119	5	15	93	6	96	22	82	173
I	S3	Bwcb	100–135	20	105	6	13	92	3	68	18	84	170
	S4	C1	135–170	20	103	5	8	78	1	40	12	33	131
	S5	C2	170–185	24	110	6	12	109	3	71	27	56	262
	S6	2Bcb	185–201	21	150	15	19	111	6	120	23	113	162
	S7	2Bcssb1	201–225	21	154	24	20	114	6	132	24	113	145
II	S8	2Bcssb2	225–271	24	178	21	21	125	7	139	28	124	146
	S9	2Bckb1	271–335	20	155	26	18	126	6	136	23	120	130
	S10	2Bckb2	335–365	26	185	22	21	156	6	145	28	126	138
	S11	3Bcb	365–377	22	120	32	19	170	5	117	20	97	123
III	S12	4Ab1	377–385	19	155	27	18	129	6	134	20	124	119
	S13	4Ab2	385–445	22	181	19	21	131	8	130	27	116	185
	S14	5Ab	445–475	24	159	13	16	131	8	97	33	84	310
IV	S15	5Bwcb	475–525	23	122	19	15	119	7	96	28	81	260
	S16	6Bcb	525–545	21	95	25	17	158	5	90	28	69	243

4.3 Radiocarbon dating (^{14}C)

The studied sequence contained very few materials suitable for radiocarbon dating: the uppermost sample was represented by charred carbon fragments of the sample S6 (Fig. 2); an intermediate sample was a large fragment of mammal bone that was lying between S9 and S10, while the deepest material was represented by a burnt tree trunk collected at the same stratigraphic level of the sample S12 (Fig. 2).

The calibrated ^{14}C dating for the three samples has been reported in Fig. 2 with 1σ confidence level, providing temporal ranges of 6660–6530, 8330–8190 and 9270–9090 y BP, which correspond to 2σ confidence level of 6720–6450, 8390–8160 and 9310–9020 y BP, respectively.

At a first instance, these values are positively correlated with a downward trend having as end-member the deepest paleosol which should have an age of ca 14–15 ky BP (see below). However, the most recent radiocarbon age (6660–6530 y BP) in horizon S6 is diachronic with the finding of Villanovan artefacts which should correspond to ca 2800–2600 y BP. The temporal gap between the radiometric age and the archaeological constraint has to be taken into account and will be discussed in the next section.

4.4 Archaeobotanical analysis

4.4.1 Pollen analysis

Pollen grains were found in all samples in a good state of preservation, allowing the identification of most of the cases. In total, 3850 pollen grains were counted from 12 sample depths. Pollen concentrations were variable depending on the richness of organic matter and the preservation conditions. They ranged from 10^2 to 10^3 p/g for most samples, and only the samples S15, S14 and S4 were comparatively poor of pollen grains (less than 10^2 p/g). The pollen flora consisted of 92 types (31 trees, shrubs, lianes and 61 herbs) and is summarized in Fig. 2. Although aware that pollen can be transported and remobilized, in our view the low dimension of the catchment implies a local (nearly in situ) origin of the grains. The sample S16 was characterized by high presence of Compositae family (81.2 %) especially *Cichorioideae* and *Asteroideae*, followed by Gramineae spontaneous group (6.7 %) with only low percentages of Pinaceae (1.8 %). *Dryas octopetala* pollen grains were also detected (1.2 %). These pollen grains indicate a landscape developed on steppic conditions (dry and cold) typical of late glacial period. The samples S15 and S14 revealed a high percentage of *Pinus*, followed by *Cichorioideae* and Gramineae spontaneous group which indicates a transition between the steppic condition delineated above and a landscape dominated by conifers, possibly occurred in the Preboreal period. The sample S13 (the lowest horizon of the third stratigraphic set), containing more pollen grains (and more pollen species), showed a drastic decrease of *Cichorioideae*, a more diversified association of *Pinus* species coupled with the appearance of *Quercus* deciduous (especially *Quercus* cf. *robur*), *Ostrya carpinifolia*,

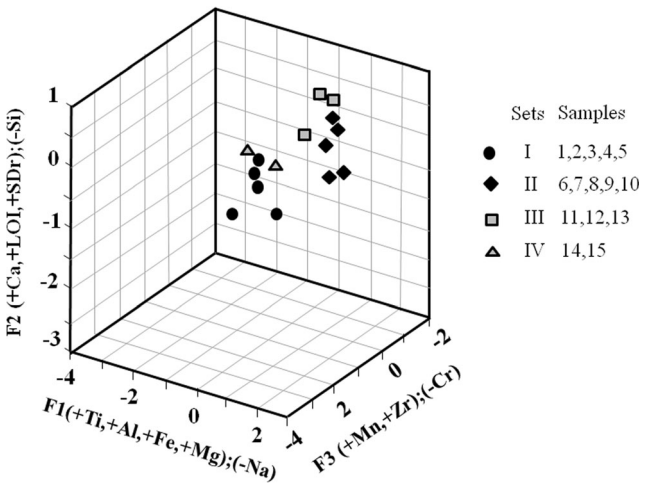

Fig. 5 3D plots of F1-F2-F3 discriminating factors obtained by the statistical elaboration of the X-ray fluorescence (XRF) geochemical data

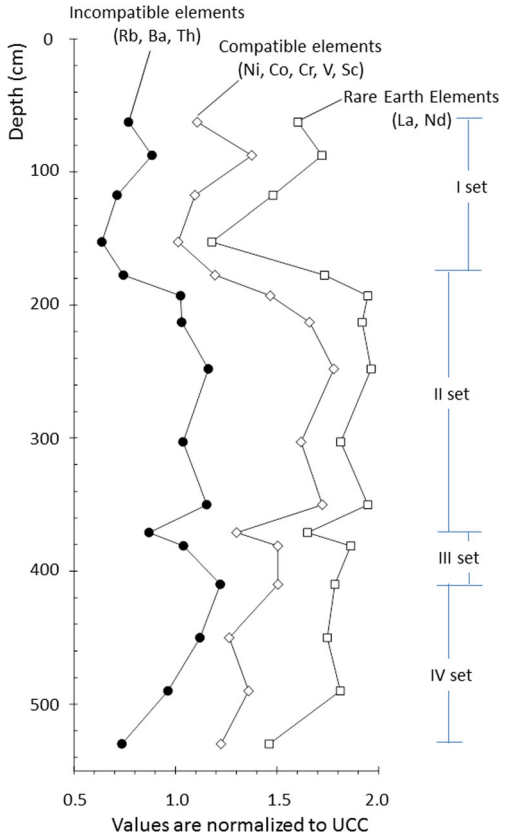

Fig. 6 Trace element content vs depth. The elements have been grouped according to their geochemical affinity and normalized to the Upper Continental Crust composition (UCC; Rudnick and Gao 2014)

Table 4 Elemental and isotopic composition of carbon obtained by EA-IRMS

	Total carbon		Organic carbon	
	(analysed at 950°)		(analysed at 450°)	
Sample	wt%	$\delta^{13}C$	wt%	$\delta^{13}C$
S1	0.92	−24.15	0.65	−24.73
S2	0.42	−24.22	0.31	−24.63
S3	0.27	−22.02	0.22	−24.45
S4	0.13	−22.70	0.13	−23.83
S5	0.17	−23.97	0.15	−24.58
S6	0.33	−24.66	0.26	−24.65
S7	0.55	−19.35	0.40	−24.76
S8	0.50	−21.53	0.37	−24.36
S9	0.76	−17.10	0.36	−24.13
S10	1.01	−16.96	0.46	−24.54
S11	1.72	−11.46	0.37	−24.78
S12	1.16	−18.78	0.57	−25.05
S13	1.01	−23.50	0.69	−25.01
S14	0.76	−23.65	0.58	−25.18
S15	0.46	−22.33	0.40	−24.41
S16	2.00	−12.99	0.36	−23.59

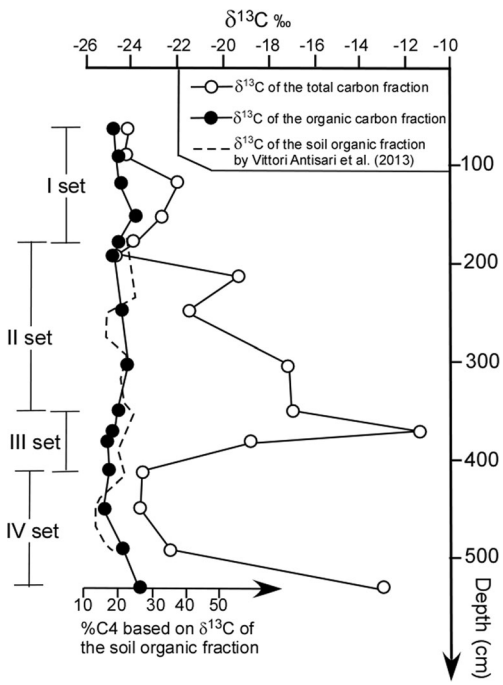

Fig. 7 Variation of $\delta^{13}C$ of the total C budget and $\delta^{13}C$ organic C fraction. The first parameter highlights the horizons containing significant amount of carbonate, whereas the second parameter gives indication on the nature of the existing vegetation that generated the organic matter

Fraxinus excelsior, *Tilia*, *Ulmus* and *Corylus*. This rich biodiversity suggests an important climatic change with the establishment of more temperate conditions. Noteworthy, this horizon corresponds to the surface where the burnt oak trees were rooted and it can be assigned to the Preboreal. The samples S12, S9 and S8 were characterized by a further increase of coniferous pollen; in particular, S12 corresponded to the part of the sequence where the burned wooden logs (9270–9090 y BP) were found. These horizons were characterized by the significant presence of Lime tree (*Tilia*) and Silver fir (*Abies alba*), which plausibly ascribe them to the Atlantic period (Accorsi et al. 1996, 2004). In the sample S9 and S8, the decrease of Pinaceae taxa was connected with an increase of *Corylus*, *Ulmus* and *Tilia*, which could suggest a weak opening in the vegetation cover. This process was accompanied by the presence or expansion of taxa indicative of human impact (e.g. Cerealia types). In the sample S6, an increase of Compositae (45.8 %) coupled with Plantaginaceae, Ranunculaceae and Sparganiaceae/Typhaceae and also Gramineae spontaneous group and Leguminosae (about 4.2 % for each species) has been observed. The vegetation suffered a further sharp change in correspondence of the first—more surficial—stratigraphic set (e.g. sample S2), where it can be observed an additional anthropogenic influence demonstrated by high Cerealia types diffusion with the presence of pollen grains of both *Hordeum* and *Avena-Triticum* groups, together with pollen grains ascribed to *Triticum* cf, *spelta* and *Secale cereal*. Further proxies of human activities were represented by Chenopodiaceae and *Plantago*, *Rumex*, *Urtica dioica* species (Li et al. 2008).

4.4.2 Microanthracological analysis

Among the 12 studied samples, the total micro-charcoal concentration of 10 samples was lower than 0.5 mm^2/g; this concentration plausibly represents representing the local background. Samples S13 and S12 contain a decidedly higher micro-charcoal concentration (8.9 and 4.9 mm^2/g, respectively). Micro-charcoal grains in S13 were characterized by 10–125 μm and is ascribed to a regional fire event, whereas micro-charcoal grains in S12 contain both the 10–125 and >125 μm size classes possibly indicating a local fire event. Therefore, the local, direct burning effect is highlighted by sample S12, whereas the evidence of sample S13 could be assigned to an independent (older) burning effects from a neighbouring area and/or to post-depositional processes reworking the grains of the overlying horizons.

4.4.3 Anthracological analysis

The charcoal analysed comes from 26 burnt trunks; generally the charcoal was found in a better state of preservation. The anthracological flora include two taxa: *Quercus* cf. *robur* (16

anthracological records) and *Quercus* undiff. (6 anthracological records); four anthracological remains are not undeterminable. All of them are regional deciduous oaks.

5 Discussion

5.1 Integration of the results

The studied soil sequence developed in an alluvial environment along the PSF longitudinal axis generated by a few kilometres-scale catchment. The depositional record stretches back to the last part of the Lateglacial period, as indicated by the integration of pollen, radiocarbon dates and soil formation.

The sedimentation rates in the studied site were calculated using the sediment thickness and the chronological data (Fig. 2; Table 1). In these calculations, we considered the radiocarbon ages, the conventional ages of 14.5 ky BP for the Bølling paleosol, 3 ky BP for the Iron Age and 2 ky BP for the top of the natural sequence. The sedimentation rates (mm/year) resulted to be 0.2 during Late-Glacial and Boreal (samples S15 to S12), 0.8 during Boreal/Atlantic (Mesolithic, samples S12 to S9) and 0.7 during the Atlantic (samples S9 to S6). The sedimentation rate further increased in the first stratigraphic set (up to 1.4 mm/year), as constrained by archaeological artefacts found between the horizons corresponding to samples S6 and S5 having ca 3 and 2 ky, respectively. Although aware that estimations can be influenced by the Sadler effect, implying lowering of the sedimentation rates for investigation of longer/older time spans (Bianchini et al. 2014), we suggest that in the studied sequence a significant increase of the sedimentation rate occurred since the Mesolithic. The high sedimentation rate recorded during the Boreal/Atlantic period implies a higher erosion rate within the Pontebuco stream catchment, preferentially affecting the outcropping area of the *Argille Azzurre* Formation (marly-clays). The more marked sediment supply to the Pontebuco stream, in turn favoured a more effective aggradation of PSF. These conditions were probably triggered by higher precipitations.

The basal sample S16 characterized by significant amount of geogenic carbonate (high percentage of Ca and Sr) and by the presence of pioneer herbaceous taxa usually considered "aridity markers" (i.e. *Artemisia*) coupled with *D. octopetala* suggests a cold and arid environment. In our view, S16 can be attributed at least to the Older Dryas period (ca. 15 ky BP) for its stratigraphic location below the horizon S15 which is characterized by typical Bølling soil features. This steppic vegetation is recorded in numerous regional pollen records of the same time period (Watts et al. 1996; Magri and Sadori 1999; Ammann et al. 2000; Denefle et al. 2000; von Grafenstein et al. 2000; Allen et al. 2002; Kotthoff et al. 2008; Bordon et al. 2009; Combourieu-Nebout et al. 2009; Fletcher et al. 2010; Desprat et al. 2013) indicating that cold-arid climate conditions were prevailing over the Mediterranean area and especially in the continental part of the Padanian basin. In fact, the overlying soil S15 can be considered a stratigraphic marker assigned to the final part of the Bølling period (ca. 15–14 ky BP) related to more wet and warm climate conditions (Frisia et al. 2005; Baroni et al. 2006; Köhler et al. 2014). It is well known that similar climatic conditions have led to the development of Xeralf (Soil Survey Staff 2014) named in Emilia-Romagna Region as *Vignola Unit soil* (Gasperi et al. 1989). These paleosols were found along the Apennine chain foothill (Cremonini et al. 2012), in the pedealpine (Cremaschi 1987; Ravazzi et al. 2012; Cremaschi and Nicosia 2012) as well as in the north-eastern part of the Padanian plain (Donnici et al. 2011). The increase of *Pinus* indicates a vegetation transition between steppic environment toward a landscape dominated by conifers that can be associated to the formation of Alfisols under natural wood cover and xeric pedoclimate conditions (Cremaschi and Nicosia 2012). The dark (S14) and reddish (S15) horizons formed a pedosequence composed by 5Ab and 5Bwcb characterized by few pollen grains. The scarce presence of pollens should indicate a climatic transition occurred in the Younger Dryas/Preboreal period. In spite of a relative paucity of pollens, the very dark S14 sample had high content of elemental C that was detected by a misfit between C_{tot} and that calculated by (C_o+C_i). This deficiency (ΔC) can be allocated to black (elemental) charred carbon related to fires and biomass burning. Similar dark soils were found in other sites of the Emilia-Romagna Region (e.g. Alessio et al. 1980; Ravazzi et al. 2006; Cremonini et al 2007), also in distal plain facies such as probably the *Argille di Vedrana*, and although they are not all strictly coeval, they could be interpreted as pedomarkers developed between Younger Dryas and Boreal chronozones (Ammann et al. 2000; von Grafenstein et al. 2000). In the city of Bologna, a pollen sterile black-soil of similar thickness was radiocarbon dated at 9300–8650 cal BP (Cremonini et al. 2007; Cremonini et al 2012; Amorosi et al. 2014). The S13 sample (4Ab2 horizon) in the third stratigraphic set corresponds to the surface where the burnt oak trees were rooted and can be assigned to the Preboreal/Boreal period, as also suggested by the burned oak trunk of S12 horizon dating ~9.1 ky BP. The pollens in the S12 sample suggest that vegetal cover progressively developed during the Holocene (Accorsi et al. 1999) in the Boreal to Atlantic time interval. This horizon also records evidence of charred material, given by the occurrence of relics of combusted oak trees, as also confirmed by the ΔC parameter indicating the presence of elemental carbon. This suggests the occurrence of fires and biomass burning, possibly resulting from man-made deforestation practices, as suggested for other sites of northern Italy (Vescovi et al. 2010). The above lithological discontinuity (S11 sample), which marked the upper limit of the third set, suggests a sharp variation toward warmer conditions attested by the decline of *Picea* and *Abies* and the increase of

Tiliaceae. This climatic change is coupled with the above-mentioned anthropogenic influence testified by several evidence of biomass burning. These findings are in agreement with several anthropogenic indicators of early Neolithic settlement (ca. 8000 y cal BP) in many Italian sites (Bellini et al. 2009; Rottoli and Castiglioni 2009; Joannin et al. 2013).

In the investigated site of S. Lazzaro, relatively homogeneous environmental conditions persisted for a long period until the formation of sample S6, which in spite of the comparatively old radiometric age of ~6550 y BP also represented a topographic surface of the first Iron Age (Villanovan). In other words, the existence of charcoal dating to ~6550 y BP in this layer implies that this surface could have been exposed to the atmosphere for ~3500 years between the Neolithic and the Iron Ages. In spite of the long soil development, the upper part of soil profile is missing and ~30 cm of surficial horizons (A) are totally lacking, thus marking a significant erosional process.

This interpretation is coherent with the paleogeographic reconstruction provided by palynology, which indicates a change of pristine forest condition with appearance of plants introduced by human activities. The stable isotopic values of organic C are similar to those recorded by Vittori Antisari et al. (2013) in a neighbouring excavation (down to a depth of 4.5 m) which recorded soil samples having $\delta^{13}C$ between −23.8 and −26.6‰ (Fig. 7). These isotopic values on the soil organic fraction are obviously related to the type of existing vegetation, and according to Meier et al. (2014), a similar $\delta^{13}C$ range reflects a clear predominance (~80 %) of plants having C3 photosynthetic pathway. A further abrupt change is testified by the different features recorded in the most superficial horizons between the S5 and S1 samples forming the first set. The textural, mineralogical and geochemical data of these layers indicate that the source of detritus was displaced toward an area dominated by the *Sabbie di Imola* Formation (IMO, quartz-rich sands) and older soils resembling those currently recognized in the terraces of the basin (AES_6, Fig. 1b). The related soil profile appears to be very poorly developed, probably indicating continuous sedimentation pulses arriving through the time. During this period, the *Pontebuco stream* experienced high energy sheet-floods as demonstrated by the S4 sample containing unclassed pebbles and gravel. Subsequently, the PSF area suddenly become quiescent and terminated its aggradation, probably due to human intervention aimed to minimize the flood risks for the human settlement. This happened during Roman times.

5.2 Human impact on the environment

The natural and human impact on the environment is very problematic to be defined. Often, the climate is recognized as the prevailing factor (e.g. Jalut et al. 2009); however, in some cases, the mankind activities are interpreted as the prominent cause since the Holocene (Ruddiman 2003) or even starting in older periods (Tzedakis 2010). River catchments generally provide physiographic units on which the interplay of climate factors and human activities can be recognized (Arnaud-Fassetta 2011; Zanchetta et al. 2013). The vegetation development and dynamics can represent a further proxy, as biological reaction after a period of degradation (even on a bare topographic surface) can be very fast (Etienne and Corenblit 2013). The existence of florid vegetation cover generally prevents soil erosional processes, in turn promoting sedimentary inactivity. In the considered study case, the reddened soil horizon (Alfisol S15) can be considered the proof of a geomorphological stasis with limited sediment supply in the PSF area. Very high sedimentation rate appeared starting from the Mesolithic up to Neolithic, and the sedimentation took place in a distal part of the PSF, highlighting a severe change in the relationships existing between the mountain catchment and the outer plain. Interpretation needs to take into account the available paleoclimate reconstructions. Various minor climatic pulses were proposed at various spatial scales for the Holocene from all over the world: 9–8, 6–5, 4.2–3.8, 3.5–2.5, 1.2–1 and 0.6–0.15 cal yr B.P (Mayewski et al. 2004). In particular, the 8.2-ky BP cold event (Alley et al 1997), lasting 300–400 years (Barber et al. 1999), has been proposed as the natural factor triggering the inception of the Mesolithic/Neolithic transition at least in the Near and Middle East areas (Berger and Guilaineb 2009), and noteworthy this period is recorded by the intermediate ^{14}C dating (8330–8190 cal BP) of the San Lazzaro site. If attention is focussed on the chronological schemes and palaeoclimatic interpretations proposed for Northern Italy and Europe (Magny et al. 2012, 2013), it becomes striking that the Mesolithic to Neolithic aggradation phase of PSF developed during a period of relative low rainfall, possibly suggesting additional (anthropogenic?) erosional causes. Noteworthy, alluvial fans, such as PSF, represent ideal archives preferentially preserving environmental changes, whereas wider alluvial plains quickly subsiding bury the evidences and are more resilient to perturbations, i.e. less sensitive to the described variations. The presented data therefore provide fresh insights for the ongoing debate on the land-use during the Mesolithic and Neolithic, an extremely controversial topic. The slash-and-burn practice for natural wood clearance (Butzer 1982) is usually linked to the Neolithic period (Branch and Marini 2014). In particular in Emilia region, the Chalcolithic recorded the beginning of a severe human impact on the landscape (Cremaschi et al. 2011; Zanchetta et al. 2013), which is related to hunter-gatherers burning practices, as documented for other primitive communities (Tolksdorf et al. 2014). A debated question is when these practices started and the human intentionality (Gerlach et al. 2012; Guido et al. 2013; Grant et al. 2014). In our study case, the vegetation burning seems to have a local dimension plausibly linked to hunter-gatherer activities,

possibly to promote the hunting in cleared areas attracting the game (Davies et al. 2005) and/or to favour the growth of edible plant species such as acorn (Mason 2000) or hazelnut (Bos and Urz 2003). The field evidences are (i) presence micro-charcoals deriving from wood combustion, (ii) isotopic evidence (ΔC) which suggests the presence of elemental carbon probably supplied by very fine particles not recorded by optical observation and (iii) the record of a combusted oak wood quickly substituted by edible plant assemblages. These indications, suggesting the repetitive occurrence of fires and biomass burning in three contiguous stratigraphic units, allow us to exclude the causality of the burning and support a man-made origin. The intentional production of fires is also suggested by the absence of charcoal within the Bølling horizon formed during a warm phase, and their concentration in soils formed during a relatively wetter period in the time interval 9.5–7 ky cal BP. On this basis, we propose that in the S. Lazzaro site the human impact on the environment predated by more than 1 ky what recorded in the Liguria Apennine (Guido et al. 2013) or Tuscany (Colombaroli et al. 2008). Although a human role on the observed vegetation changes cannot be demonstrated, it has to be remarked the presence of species providing edible fruit since 9 ky BP, a fact that could imply the occurrence of plant selection and concentration. Similar hypothesis have been proposed by Zeder (2008) for various sites of the Mediterranean area. These early activities, although not related to conscious agricultural practices could be effective in promoting the soil erosion within the catchment, as demonstrated the measured sedimentation rates. On the other hand, more intentional agricultural activities started much later, possibly in connection with the onset of cereals that in studied site appeared only in the Chalcolithic.

6 Conclusions

The presented data emphasize the importance of alluvial sediment and soil investigations to elucidate fluctuations of environmental conditions, including climatic changes and past anthropogenic impacts on the natural landscape. In particular, the considered stratigraphic sequence exposed in the locality of San Lazzaro di Savena (Bologna, Italy) provides information on the Lateglacial-Holocene evolution of the northern foot-hill Apennine area, suggesting that at the beginning of this period the climate was quite cold and relatively arid favouring a steppic vegetation growth. With the Holocene inception, a slight increase in the temperature and a relative increase of precipitations favoured the development of forest constituted by abundant conifers. Humans impacted this environment making fires during the Mesolithic to clear the area and during the Neolithic to obtain soils for agriculture and animal farming. The human presence favoured geomorphological and hydraulic instabilities, accelerating soil erosion. Therefore, the observed data suggest that human impact on the landscape started to be effective in the Mesolithic period, earlier than usually considered by previous studies. Finally, more recent (probably Roman age) hydraulic works confined the *Pontebuco stream* leading to the inactivation of his alluvial fan area, rendering the surrounding lands stable for settlements.

Acknowledgments A special thank must be addressed to Giuliana Steffè and Valentina Manzelli (Soprintendenza Archeologica dell'Emilia-Romagna) and to C. Mazzoni (Soc. Coop. Archeologia) for the helpful discussion. The authors are also grateful to R. Tassinari that carried out the XRF analyses at the University of Ferrara. The authors thank Dr. R. Tassinari for the analytical support, and referees and editors for their constructive comments that helped to improve earlier versions of this manuscript.

References

Accorsi CA, Bandini Mazzanti M, Mercuri AM, Rivalenti C, Trevisan Grandi G (1996) Holocene forest pollen vegetation of the Po plain—Northern Italy (Emilia Romagna data). Allionia 34:233–276

Accorsi CA, Bandini Mazzanti M, Forlani L, Mercuri AM, Trevisan Grandi G (1999) An overview of Holocene forest pollen flora/vegetation of the Emilia Romagna region—Northern Italy. Archivio Geobotanico 5:3–27

Accorsi CA, Bandini Mazzanti M, Forlani L, Mercuri AM, Trevisan Grandi G (2004) Holocene forest vegetation (pollen) of the Emilia Romagna Plain—Northern Italy. Colloques Phytosociologiques 28: 1–103

Alessio M, Allegri L, Bella E, Calderoni G, Cortesi G, Cremaschi M, Improta S, Papani G, Petrone V (1980) Le datazioni ^{14}C della pianura tardo-wurmiana ed olocenica nell'Emilia occidentale. Contributi preliminari alla realizzazione della Carta Neotettonica d'Italia (P.F. Geodinamica). Pubbl n 356:1411–1435

Allen JRM, Watts WA, McGee E, Huntley B (2002) Holocene environmental variability—the record from Lago Grande di Monticchio, Italy. Quatern Int 88:69–80

Alley RB, Mayewsky PA, Sowers T, Stuiver M, Taylor KC, Clark PU (1997) Holocene climatic instability: a prominent, widespread event 8200 yr ago. Geology 25:483–486

Ammann B, Birks HJB, Brooks SJ, Eicher U, von Grafenstein U, Hofmann W, Lemdahl G, Schwander J, Tobolski K, Wick L (2000) Quantification of biotic responses to rapid climatic changes around the Younger Dryas—a synthesis. Palaeogeogr Palaeoclimatol Palaeoecol 159:313–347

Amorosi A, Farina M, Severi P, Preti D, Caporale L, Di Dio G (1996) Genetically related alluvial deposits across active fault zones: an example of alluvial fan-terrace correlation from the upper Quaternary of the southern Po Basin, Italy. Sediment Geol 102: 275–295

Amorosi A, Caporale L, Cibin U, Colalongo ML, Pasini G, Ricci Lucchi F, Severi P, Vaiani SC (1998) The Pleistocene littoral deposits (*Imola Sands*) of the Northern Apennines piedmont. Giorn Geol 60:83–118

Amorosi A, Bruno L, Rossi V, Severi P, Hajdas I (2014) Paleosol architecture of a late Quaternary basin-margin sequence and its implications for high-resolution, non-marine sequence stratigraphy. Global Planet Change 112:12–25

Anderson DG, Maasch KA, Sandweiss DH, Mayewski PA (2007) Climate and culture change: Exploring Holocene transitions.

Climate Change and Cultural Dynamics, A Global Perspective on Mid-Holocene Transitions, pp 1-23
Arnaud-Fassetta G (2011) L'histoire des vallées, entre géosciences et géoarchéologie. Méditerranée 117:25–34
Barber C, Dyke A, Hillaire-Marcell C, Jennings AE, Andrews JT, Kerwin MW, Bilodeau G, Mcneely R, Southon J, Morehead MD, Gagnon JM (1999) Forcing the cold event of 8,200 years ago by catastrophic drainage of Laurentide lakes. Nature 400:344–348
Baroni C, Zanchetta G, Fallick AE, Longinelli A (2006) Mollusca stable isotope record of a core from Lake Frassino, northern Italy: hydrological and climatic changes during the last 14 ka. The Holocene 16: 827–837
Bell M, Walker MJC (2005) Late Quaternary environmental change: physical and human perspectives (2nd edition). Second Edition Pearson and Prentice Hall, Harlow, UK, 348 pp
Bellini C, Mariotti-Lippi M, Montanari C (2009) The Holocene landscape history of the NW Italian coasts. The Holocene 19:1161–1172
Berger J-F, Guilaineb J (2009) The 8200calBP abrupt environmental change and the Neolithic transition: a Mediterranean perspective. Quatern Int 200:31–49
Berglund BE, Ralska-Jasiewiczowa M (1986) Pollen analysis and pollen diagrams. In: Berglund BE (ed) Handbook of Holocene Palaeoecology and Palaeohydrology. Wiley, Chichester, pp 455–484
Beug HJ (2004) Leifaden der Pollenbestimmungen fur Mitteleuropa and angrenznde Gebiete. Verlag Friedrich Pfeil, Munich, p 54
Bianchini G, Cremonini S, Di Giuseppe D, Vianello G, Vittori Antisari L (2014) Multiproxy investigation of a Holocene sedimentary sequence near Ferrara (Italy): clues on the physiographic evolution of the eastern Padanian plain. J Soils Sediments 14:230–242
Blackwell PG, Buck CE, Reimer P (2006) Important features of the new radiocarbon calibration curves. Quaternary Sci Rev 25:408–413
Boccaletti M, Corti G, Martelli L (2011) Recent and active tectonics of the external zone of the northern Apennines (Italy). Int Jour Earth Sci (Geol Rundschau) 100:1331–1348
Bordon A, Peyron O, Lézine A, Brewer S, Fouache E (2009) Pollen-inferred Late-Glacial and Holocene climate in southern Balkans (Lake Maliq). Quatern Int 200:19–30
Bos JAA, Urz R (2003) Late Glacial and early Holocene environment in the middle Lahn river valley (Hessen, central-west Germany) and the local impact of early Mesolithic people—pollen and macrofossil evidence. Vegetation History and Archaeobotany 12:19–36
Branch NP, Marini NAF (2014) Mid-Late Holocene environmental change and human activities in the northern Apennines, Italy. Quatern Int 353:34–51
Bronk Ramsey C (2001) Development of the Radiocarbon Program OxCal. Radiocarbon 43:355–363
Butzer KW (1982) Archaeology as human ecology. Cambridge University Press, Cambridge, **364 p**
Calcagnile L, Quarta G, D'Elia M (2005) High resolution accelerator-based mass spectrometry: precision accuracy and background. Appl Radiat Isotopes 62:623–629
Clark RL (1982) Point count estimation of charcoal in pollen preparations and thin sections of sediment. Pollen Spores 24:523–525
Clark JS, Patterson WA III (1997) Background and local charcoal in sediments: scales of fire evidence in the paleorecord. In: Clark JS, Cachier H, Goldammer JG, Stocks B (eds.) Sediment records of biomass burning and global change. NATO ASI Series 1: Global Environmental Change, 51, Springer, Berlin, 23–48
Colombaroli D, Vanniere B, Chapron E, Magny M, Tinner W (2008) Fire–vegetation interactions during the Mesolithic-Neolithic transition at Lago dell'Accesa, Tuscany, Italy. The Holocene 18:679–692
Combourieu-Nebout N, Peyron O, Dormoy I, Desprat S, Beaudouin C, Kotthoff U, Marret F (2009) Rapid climatic variability in the west Mediterranean during the last 25 000 years 25 from high resolution pollen data. Clim Past 5:503–521
Cremaschi M (1987) Paleosols and vetusols in the central Po Plain (Northern Italy). A study in Quaternary geology and soil development. Unicopli, Milano, p 306
Cremaschi M, Nicosia C (2012) Sub-Boreal aggradation along the Apennine margin of the Central Po Plain: geomorphological and geoarchaeological aspects. Geologija 2:155–174
Cremaschi M, Nicosia C, Salvioni M (2011). L'uso del suolo nell'Eneolitico e nel Bronzo antico, nuovi dati dalla Pianura Padana centrale. L'età del Rame in Italia - Atti della XLIII Riunione Scientifica dell'Istituto Italiano di Preistoria e Protostoria (2008):225-231
Cremonini S (2014) La transizione geomorfologica "catena-pianura" nella città di Bologna. Osservazioni per un'analisi evolutiva dell'areale del santuario etrusco di Villa Cassarini nell'arco cronologico pre-protostorico e classico. In Romagnoli S (ed.), Il santuario etrusco di Villa Cassarini a Bologna, Bonomia University Press, pp 34–58
Cremonini S, Lorito S, Vianello G, Vittori Antisari L, Fusco F (2007) Suoli olocenici sepolti nel centro urbano di Bologna. Prime considerazioni pedologiche e radiometriche. Boll Società Italiana della Scienza del Suolo 56:48–56
Cremonini S, Falsone G, Marchesini M, Vinello G, Vittori Antisari L (2012) Suoli olocenici sepolti nell'Emilia orientale—Holocene buried soils in Eastern Emila Region. EQA (Environmental Quality-Qualità ambientale) 1: 107–121. (ISSN 2039-9898)
Davies P, Robb JG, Ladbrook D (2005) Woodland clearance in the Mesolithic: the social aspect. Antiquity 79(304):280–288
Denefle M, Lezine AM, Fouache E, Dufaure JJ (2000) A 12 000 yr pollen record from Lake Maliq, Albania. Quaternary Res 54:423–432
Desprat S, Combourieu-Nebout N, Essallami L, Sicre MA, Dormoy I, Peyron O, Siani G, Bout Roumazeilles V, Turon J (2013) Deglacial and Holocene vegetation and climatic changes in the southern Central Mediterranean from a direct land-sea correlation. Clim Past 9:767–787
Di Giuseppe D, Bianchini G, Faccini B, Coltorti M (2014) Combination of wavelength dispersive X-ray fluorescence analysis and multivariate statistic for alluvial soils classification: a case study from the Padanian Plain (Northern Italy). X-Ray Spectrom 43:165–174
Diamond J (2005) Collapse: how societies choose to fail or succeed. Viking Press, New York, pp 137–155
Donnici S, Serandrei-Barbero R, Bini C, Bonardi M, Lezziero A (2011) The caranto paleosol and its role in the early urbanization of Venice. Geoarchaeology 26:514–543
Etienne S, Corenblit D (2013) Biogeomorphologie de la France. Mercier D (ed.), Geomorphologie de la France, Paris :157-170
Facchinelli A, Sacchi E, Mallen L (2001) Multivariate statistical and GIS approach to identify heavy metal sources in soils. Environ Pollut 114:313–324
Faegri K, Iversen J (1989) Textbook of Pollen Analysis, 4th edition. Chichester, John Wiley & sons, pp 328
Farabegoli E, Rossi Pisa P, Costantini B, Gardi C (1994) Cartografia tematica per lo studio dell'erosione a scala di bacino. Rivista di Agronomia 28:356–363
Fiorentino G, Caracuta V, Calcagnile L, D'Elia M, Matthiae P, Mavelli F, Quarta G (2008) Third millennium B.C. climate change in Syria highlighted by carbon stable isotope analysis of ^{14}C-AMS dated plant remains from Ebla. Palaeogeogr Palaeocl 266:51–58
Fleitmann D, Burns SJ, Mangini A, Mudelsee M, Kramers J, Villa I, Neff U, Al-Subbary AA, Buettner A, Hippler D, Matter A (2007) Holocene ITCZ and Indian monsoon dynamics recorded in stalagmites from Oman and Yemen (Socotra). Quaternary Sci Rev 26: 170–188
Fletcher WJ, Sanchez Goñi MF, Peyron O, Dormoy I (2010) Abrupt climate changes of the last deglaciation detected in a Western Mediterranean forest record. Clim Past 6:245–264

Frisia S, Borsato A, Spotl C, Villa I, Cucchi F (2005) Climate variability in the SE Alps of Italy over the past 17000 years reconstructed from a stalagmite record. Boreas 34:445–455

Gasperi G, Cremaschi M, Mantovani Uguzzoni MP, Cardarelli A, Cattani M, Labate D (1989) Evoluzione plio-quaternaria del margine appenninico modenese e dell'antistante pianura. Note illustrative alla carta geologica. Mem Soc Geol It 29:375–431

Gee GW, Bauder JW (1986) Particle-size analysis. In: Klute A. (ed.), Methods of soil analysis, part 1, Second edition. Number 9 of the series Agronomy. ASA and SSSA, Madison WI, USA, pp 383–411

Gerlach R, Fischer P, Eckmeier E, Hilgers A (2012) Buried dark soil horizons and archaeological features in the Neolithic settlement region of the Lower Rhine area, NW Germany: formation, geochemistry and chronostratigraphy. Quatern Int 265:191–204

Giraudi C, Magny M, Zanchetta G, Drysdale RN (2011) The Holocene climatic evolution of Mediterranean Italy: a review of the continental geological data. The Holocene 21:105–115

Grant MJ, Hughes PDM, Barber KE (2014) Climatic influence upon early to mid-Holocene fire regimes within temperate woodlands: a multi-proxy reconstruction from the New Forest, southern England. J Quaternary Sci 29:175–188

Grosser D (1977) Die Holzer Mitteleuropas. Ein Mikrophotographischer Lehratlas. Springer, Berlin

Guido MA, Menozzi BI, Bellini C, Placereani S, Montanari C (2013) A palynological contribution to the environmental archaeology of a Mediterranean mountain wetland (North West Apennines, Italy). The Holocene 23:1517–1527

Hather JG (2000) The identification of the northern European woods. A guide for archaeologists and conservators. Archetype Publications, London

Jacquiot C, Trenard Y, Dirol D (1973) Atlas d'anatomie des bois d'Angiospermes, vol 1–2. Centre Technique du bois, Paris

Jalut G, Dedoubat JJ, Fontugne M, Otto T (2009) Holocene circum-Mediterranean vegetation changes: climate forcing and human impact. Quat Int 200:4–18

Joannin S, Vannière B, Galop D, Peyron O, Haas JN, Gilli A, Chapron E, Wirth SB, Anselmetti F, Desmet M, Magny M (2013) Climate and vegetation changes during the Lateglacial and early-middle Holocene at Lake Ledro (southern Alps, Italy). Clim Past 9:913–933

Jolliffe IT (2002) Principal Component Analysis. Springer, New York, **488 pp**

Köhler P, Knorr G, Bard E (2014) Permafrost thawing as a possible source of abrupt carbon release at the onset of the Bølling/Allerød. Nat Commun 5(5520):1–10

Kotthoff U, Pross J, Muller UC, Peyron O, Schmiedl G, Schulz H (2008) Climate dynamics in the borderlands of the Aegean Sea during formation of Sapropel S1 deduced from a marine pollen record. Quaternary Sci Rev 27:832–845

Lenzi F, Nenzioni G (1996) Lettere di pietra. I depositi pleistocenici: sedimenti, industrie e faune del margine appenninico bolognese. Bologna, 1–867

Li YY, Zhou LP, Cui HT (2008) Pollen indicators of human activity. Chinese Sci Bull 53:1281–1293

Loeppert RH, Suarez DL (1996) Carbonate and gypsum. In: Sparks DL (ed) Method of soil analysis, Part 3rd edn, Chemical methods. SSSA and ASA, Madison, pp 437–474

Lowe JJ, Accorsi AC, Bandini Mazzanti M, Bishop A, Van der Kaars S, Forlani L, Mercuri AM, Rivalenti C, Torri P, Watson (1996) Pollen stratigraphy of sediment sequences from crater lakes Albano and Nemi (near Rome) and from the central Adriatic, spanning the interval from oxygen isotope stage 2 to the present day. Memorie Istituto Italiano Idrobiologia 55:71–98

Magny M, De Beaulieu JL, Drescher-Schneider R, Vannière B, Walter-Simonnet AV, Millet L, Bossuet G, Peyron O (2006) Climatic oscillations in central Italy during the Last Glacial-Holocene transition: the record from Lake Accesa. J Quaternary Sci 21:311–320

Magny M, Peyron O, Sadori L, Ortu E, Zanchetta G, Vanniere B, Tinner W (2012) Contrasting patterns of precipitation seasonality during the Holocene in the south- and north central Mediterranean. J Quat Sci 27:290–296

Magny M, Combourieu-Nebout N, de Beaulieu JL, Bout-Roumazeilles V, Colombaroli D, Desprat S, Francke A, Joannin S, Ortu E, Peyron O, Revel M, Sadori L, Siani G, Sicre MA, Samartin S, Simonneau A, Tinner W, Vanniere B, Wagner B, Zanchetta G, Anselmetti F, Brugiapaglia E, Chapron E, Debret M, Desmet M, Didier J, Essallami L, Galop D, Gilli A, Haas JN, Kallel N, Millet L, Stock A, Turon JL, Wirth S (2013) North–south palaeohydrological contrasts in the central Mediterranean during the Holocene: tentative synthesis and working hypotheses. Clim Past 9:2043–2071

Magri D, Sadori L (1999) Late Pleistocene and Holocene pollen stratigraphy at Lago di Vico (central Italy). Veget Hist Archaeobot 8:247–260

Martelli L, Amorosi A, Severi P (2009) Note illustrative della Carta Geologica d'Italia alla scala 1:50.000. Foglio 221-Bologna, Roma, 127 pp

Mason SLR (2000) Fire and Mesolithic subsistence-managing oaks for acorns in northwest Europe? Palaeogeogr Palaeoclimatol Palaeoecol 164:139–150

Mayewski PA, Rohling EE, Stager JC, Karlén W, Maasch KA, Meeker LD, Meyerson EA, Gasse F, van Kreveld S, Holmgren K, Lee-Thorp J, Rosqvist G, Rack F, Staubwasser M, Schneider RR, Steig EJ (2004) Holocene climate variability. Quat Res 62:243–255

Meier HA, Driese SG, Nordt LC, Forman SL, Dworkin SI (2014) Interpretation of Late Quaternary climate and landscape variability based upon buried soil macro- and micromorphology, geochemistry, and stable isotopes of soil organic matter, Owl Creek, central Texas, USA. Catena 114:157–168

Miller GH, Brigham-Grette J, Alley RB, Anderson L, Bauch HA, Douglas MSV, Edwards ME, Elias SA, Finney BP, Fitzpatrick JJ, Funder SV, Herbert TD, Hinzman LD, Kaufman DS, MacDonald GM, Polyak L, Robock A, Serreze MC, Smol JP, Spielhagen R, White JWC, Wolfe AP, Wolff EW (2010) Temperature and precipitation history of the Arctic. Quaternary Sci Rev 29:1679–1715

Moore PD, Webb JA, Collinson ME (1991) Pollen analysis, 2nd edn. Blackwell, Oxford

Natali C, Bianchini G (2015) Thermally based isotopic speciation of carbon in complex matrices: a tool for environmental investigation. Environ Sci Pollut Res 22:12162–12173

Nenzioni G (1985) Testimonianze mesolitiche, neolitiche e delletà del Rame dal territorio di S. Lazzaro di Savena. In: Lenzi F, Nenzioni G, Peretto C (eds) Materiali e documenti per un museo della preistoria. S. Lazzaro di Savena e il suo territorio, Bologna, pp 211–250

Patterson WA III, Edwards KJ, MacGuire DJ (1987) Microscopic charcoal as a fossil indicator of fire. Quat Sci Rev 6:3–23

Picotti V, Pazzaglia FJ (2008) A new active tectonic model for the construction of the Northern Apennines mountain front near Bologna (Italy). J Geophys Res 113:B08412

Picotti V, Bertotti G, Capozzi R, Fesce AM (1997) Evoluzione tettonica quaternaria della pianura padana centro-orientale e dei suoi margini. Il Quaternario 19:513–520

Pignatti S (1982) Flora d'Italia. Edagricole, Bologna

Ravazzi C, Donegana M, Vescovi E, Arpenti E, Caccianiga M, Kaltenrieder P, Londeix L, Marabini S, Mariani S, Pini R, Vai GB, Wick L (2006) A new Late-glacial site with *Picea abies* in the northern Apennine foothills: an exception to the model of glacial refugia of trees. Veget Hist Archaeobot 15:357–371

Ravazzi C, Deaddis M, De Amicis M, Marchetti M, Vezzoli G, Zanchi A (2012) The last 40 ka evolution of the Central Po Plain between the Adda and Serio rivers. Geologija 2:131–154

Rottoli M, Castiglioni E (2009) Prehistory of plant growing and collecting in Northern Italy, based on seed remains from the Early

Neolithic to the Chalcolithic (c. 5600–2100 cal B.C.). Veget Hist Archaeobot 18:91–103

Ruddiman WF (2003) The anthropogenic greenhouse era began thousands of years ago. Clim Chang 61:261–293

Rudnick RL, Gao S (2014) Composition of the continental crust. Treatise on Geochemistry (Second Edition) 4:1–51

Scarani R (1963) Repertorio di scavi e scoperte dell'Emilia e Romagna, in: "Preistoria dell'Emilia e Romagna" vol. 2, 175 -617, Bologna.

Schoeneberger PJ, Wysocki DA, Benham EC, Soil Survey Staff (2012) Field book for describing and sampling soils. Version 3.0. Natural Resources Conservation Service. National Soil Survey Center, Lincoln, NE

Schweingruber FH (1990) Anatomie europäischer Hölzer. Eidgenössische Forschungsanstalt für Wald, Schnee und Landschaft, Birmensdorf (ed). Verlag Paul Haupt, Bern and Stuttgart, 800 pp

Soil Survey Staff (2014) Keys to soil taxonomy, 12th edn. USDA-Natural Resources Conservation Service, Washington, DC

Stramondo S, Saroli M, Tolomei C, Moro M, Doumaz F, Pesci A, Loddo F, Baldi P, Boschi E (2007) Surface movements in Bologna (Po plain—Italy) detected by multitemporal DInSAR. Remote Sens Environ 110:304–316

Stuiver M, Polach HA (1977) Discussion: reporting of ^{14}C data. Radiocarbon 19:355–363

Tolksdorf JF, Turner F, Kaiser K, Eckmeier E, Bittmann F, Veil S (2014) Potential of palaeosols, sediments and archaeological features to reconstruct Late Glacial fire regimes in the northern Central Europe—case study Grabow site and overview. Z Geomorphol 58: 211–232

Tutin TG, Heywood VH, Burges NA, Moore DM, Valentine DH, Walters SM, Webb DA (eds) (1964–1993) Flora Europaea, Vols 2–5 and Vol. 1, 2nd edn. Cambridge University Press, Cambridge, UK

Tzedakis PC (2010) The MIS 11—MIS 1 analogy, southern European vegetation, atmospheric methane and the "early anthropogenic hypothesis". Clim Past 6:131–144

Vescovi E, Ammann B, Ravazzi C, Tinner W (2010) A new Late-Glacial and Holocene record of vegetation and fire history from Lago del Greppo, Northern Apennines, Italy. Veg Hist Archaeobot 19:219–233

Vittori Antisari L, Cremonini S, Desantis P, Vianello G (2011) Anthropogenic cycles in a chronosequence from the Bronze Age to Renaissance Period (Bologna, Italy). EQA 6:1–6

Vittori Antisari L, Cremonini S, Desantis P, Calastri C, Vianello G (2013) Chemical characterisation of anthro-technosols from Bronze to Middle Age in Bologna (Italy). J Archaeol Sci 40:3660–3671

von Grafenstein U, Eicher U, Erlenkeuser H, Ruch P, Schwander J, Ammann B (2000) Isotope signature of the Younger Dryas and two minor oscillations at Gerzensee (Switzerland): palaeoclimatic and palaeolimnologic interpretation based on bulk and biogenic carbonates. Palaeogeogr Palaeoclimatol Palaeoecol 159:215–229

Watts WA, Allen JRM, Huntley B (1996) Vegetation history and palaeoclimate of the Last Glacial period at Lago Grande di Monticchio, southern Italy. Quaternary Sci Rev 15:133–53

Weninger B, Clare L, Rohling EJ, Bar-Yosef O, Böhner U, Budja M, Bundschuh M, Feurdean A, Gebel H-G, Jöris O, Linstädter J, Mayewski P, Mühlenbruch T, Reingruber A, Rollefson G, Schyle D, Thissen L, Todorova H, Zielhofer C (2009) The impact of rapid climate change on prehistoric societies during the Holocene in the Eastern Mediterranean. Documenta Praehistorica XXXVI: 7–59

Whitlock C, Larsen C (2001) Charcoal as a fire proxy. Smol JP, Birks HJB, Last WM (eds) Tracking environmental change using lake sediments, 3—terrestrial, algal, and siliceous indicators. Kluwer Academic Publishers, Dordrecht, The Netherlands

Whitlock C, Millspaugh SH (1996) Testing assumptions of fire history studies: an examination of modern charcoal accumulation in Yellowstone National Park. The Holocene 6:7–15

Wiersma AP, Jongma JI (2010) A role for icebergs in the 8.2 ka climate event. Clim Dynam 35:535–549

Woodward J (2009) The physical geography of the Mediterranean. Oxford University Press, Oxford

Yu S, Colman SM, Lowell TV, Milne GA, Fisher TG, Breckenridge A, Boyd M, Teller JT (2010) Freshwater outburst from Lake Superior as a trigger for the cold Event 9300 Years Ago. Science 328:1262–1266

Zanchetta G, Bini M, Cremaschi M, Magny M, Sadori L (2013) The transition from natural to anthropogenic-dominated environmental change in Italy and the surrounding regions since the Neolithic: an introduction. Quatern Int 303:1–9

Zeder MA (2008) Domestication and early agriculture in the Mediterranean Basin: origins, diffusion, and impact. Proc Natl Acad Sci U S A 105:11597–11604